Timing Jitter in NbN Superconducting Microstrip Single-Photon Detector

D.Yu. Vodolazov,[1,2,†] N.N. Manova,[1] Yu.P. Korneeva,[1,*] and A.A. Korneev[1,3]

[1] *Physics Department, Moscow Pedagogical State University, Moscow 119991, Russia*

[2] *Institute for Physics of Microstructures, Russian Academy of Sciences, Nizhny Novgorod GSP-105, Russia*

[3] *National Research University Higher School of Economics, Moscow 101000, Russia*

(Received 10 June 2020; revised 13 September 2020; accepted 22 September 2020; published 21 October 2020)

We experimentally study timing jitter of single-photon detection by NbN superconducting strips with width w ranging from 190 nm to 3 μm. We find that timing jitter of both narrow (190 nm) and micron-wide strips is about 40 ps at currents where internal detection efficiency η saturates and it is close to our instrumental jitter. We also calculate intrinsic timing jitter in wide strips using the modified time-dependent Ginzburg-Landau equation coupled with a two-temperature model. We find that with increasing width the intrinsic timing jitter increases and the effect is most considerable at currents where a rapid growth of η changes to saturation. We relate it with complicated vortex and antivortex dynamics, which depends on a photon's absorption site across the strip and its width. The model also predicts that at current close to depairing current the intrinsic timing jitter of a wide strip could be about $\hbar/k_BT_c$ (T_c is a critical temperature of superconductor), i.e., the same as for a narrow strip.

DOI: 10.1103/PhysRevApplied.14.044041

I. INTRODUCTION

Detection of a single optical photon by a current-carrying superconducting strip was first demonstrated in Ref. [1], this type of detector was called a superconducting (nanowire) single-photon detector (SSPD or SNSPD). Since then, for a long time it was believed that only a relatively narrow superconducting strip, with width of approximately the photon-induced hotspot (region with suppressed superconductivity with typical diameter $D_{\rm HS} \sim$ 50–100 nm), can detect single photons. However, in Ref. [2] it was argued that a wide strip having width $D_{\rm HS} \ll w \lesssim \Lambda$ (Λ is the Pearl penetration depth, which could be about 100 μm for a relatively thin strip) can also detect single photons if it is biased by the current close to depairing current $I_{\rm dep}$. Recently this prediction has been experimentally confirmed in Refs. [3–6] for detectors made of NbN, MoSi, and WSi superconductors. These results pave the way to use such superconducting microstrip single-photon detectors (SMSPDs) in applications requiring large-area detectors, e.g., confocal microscopy, free-space quantum cryptography, deep-space optical communication, etc.

For different applications it is important to have small timing jitter (variance of time delay in the appearance of the voltage response after absorption of the photon). Timing jitter in SNSPD was studied both experimentally [7–13] and theoretically [14–16] and the lowest value of approximately 3 ps was reached in Ref. [13], which is much lower than the timing jitter of practical detectors [17,18].

In our work we study timing jitter in a NbN strip with width w ranging from 0.19 to 3 μm. The lowest width corresponds to SNSPD while the micron ones to SMSPD. We find that at low currents (where photon count rate increases before saturation) the probability density function (PDF) for delay time in the appearance of photon-induced voltage response becomes broader with increasing w. At relatively large currents (saturation area in dependence of photon counts on bias current) timing jitter decreases and reaches approximately 40 ps both for narrow and wide strips, which is close to our instrumental jitter. Calculations based on the modified time-dependent Ginzburg-Landau equation coupled with a two-temperature model show that the large variance in time delay at low currents (intrinsic timing jitter) could be connected with the position-dependent response and dynamics of vortices and antivortices nucleated near the hotspot in a wide strip. At large currents, the large difference in time delay disappears and intrinsic timing jitter resembles the one in a narrow strip—it drastically decreases with increasing I and could be as small as $\hbar/k_BT_c$ (T_c is a critical temperature of the superconductor) as the current approaches the depairing current.

II. EXPERIMENT

We investigate NbN strips with width varying from 0.19 to 3 μm, and the length being approximately 10

*korneeva@rplab.ru

†vodolazov@impras.ru

times the width for each sample. We use sapphire (Al_2O_3) wafer with a stack of Au and Si_3N_4 layers acting as an optical cavity [19]. The NbN film is deposited by dc reactive magnetron sputtering of niobium (Nb) target in a mixture of argon (Ar) and nitrogen (N_2). All the samples presented here are fabricated from the same film with thickness $d = 6.8$ nm, which is determined from a calibrated sputtering rate and time. The temperature dependence of resistance $R(T)$ and residual resistance ratio RRR $= R(300\text{K})/R(20\text{K})$ are measured in a four-probe configuration. For our film, the superconducting transition temperature $T_c = 9$ K and RRR $= 0.72$. The sheet resistance is calculated from the resistance of the sample and the number of squares for each sample. The theoretical depairing current I_{dep} at a given temperature is determined from the approximate expression:

$$I_{\text{dep}}(T) = 0.74\frac{w[\Delta(0)]^{3/2}}{eR_s\sqrt{\hbar D}}\left[1-(T/T_c)^2\right]^{3/2}, \qquad (1)$$

where applicability for dirty superconductors was justified by Clem and Kogan [20]. The superconducting gap at zero temperature is calculated using the BCS formula $\Delta(0) = 1.76k_BT_c$. We use diffusion coefficient $D = 0.4$ cm^2/s typical for NbN. Parameters of the studied devices are summarized in Table I. For all studied samples we estimate ratio I_c/I_{dep} in the range 0.8–0.9. This is higher compared to typical values previously reported for meanders with a 50–100-nm-wide strip, but similar to what we had in our previous research [3,4] of micron-wide strips. We attribute higher I_c/I_{dep} ratio to the absence of sharp turns leading to current-crowding effect. A similar value was also found by Frasca *et al.* [21] from direct measurement of I_{dep} in MoSi and NbN strips.

All measurements of jitter are done at $T = 1.7$ K. The detectors are mounted in a sample holder in a dipstick and connected to a transmission coaxial line. We use a precision voltage source to bias our samples and two room-temperature amplifiers Mini-Circuits ZFL-1000LN+ (1 GHz band, 46 dB total gain) to amplify the output signals to a level suitable for triggering the pulse counter and the time tagger. SNSPDs made as short strips feature low kinetic inductance, and after photon click do not switch back to superconducting state spontaneously, the effect is called "latching." To avoid latching, one may use additional inductors like in Refs. [5,6,12,13]. To prevent latching in our samples (kinetic inductance of about 1 nH), we use shunt resistors connected in parallel to the sample. We use shunts 14.6, 5.8, 5.2, 4.5 Ω for samples with widths 0.19, 1.02, 1.95, 3.00 μm, respectively. These values provide minimum jitter for each type of sample. Smaller shunt results in a smaller voltage pulse magnitude, thus reducing signal-to-noise ratio and increasing jitter. Larger shunt prevents reaching high bias current close to I_c where jitter is minimal. As in our previous work [3], here we observe a small increase of the critical current for samples with shunt. We attribute it to a trivial current division between the shunt and nonsuperconducting parts of the sample and the sample holder (contact pads, bonding wires, etc). For consistency, everywhere in this paper we renormalize sample currents by a factor of I_c/I_c^{sh}, where I_c is the critical current without the shunt, I_c^{sh} is the critical current measured on the same sample with shunt (as if the sample shows the same I_c when the shunt is installed).

Light is delivered by a single-mode optical fiber SMF28 to the sample placed at a distance of 10 cm away from the ferrule to create a uniformly illuminated field. We use a 1064-nm wavelength laser with 5-ps pulse duration, and 200-MHz repetition rate. This repetition rate does not affect the performance of the samples: first, this rate is smaller than the largest possible count rate of the samples (approximately 500 MHz), which is defined by the reciprocal recovery time (2 ns) of the sample after the photon count; second, we always use heavily attenuated laser pulses, so that not more than 1/100 of them result in detector "clicks," in other words, maximum photon count rate never exceeds 1 million counts/s. Internal detection efficiency η, which is a probability of a "click" of the device to an absorbed photon, is found as a ratio of photon counts to the incident photon flux and normalized to the absorption of the device. We assume that a plateau near I_c corresponds to 100% internal detection efficiency. The photon flux is calibrated by measuring photon count rate of a "traditional" meander-shaped NbN SNSPD with the known detection efficiency.

TABLE I. Parameters of the studied samples for temperature $T = 1.7$ K. "Width" and "Length" are the width and length of the strip, $R_s(300\text{ K})$ is the resistance per square at $T = 300$ K, $I_c(1.7\text{ K})$ is the critical currents measured without a shunt resistor, $I_{\text{dep}}(1.7\text{ K})$ is the calculated depairing current, I_c/I_{dep} is the ratio of the critical current to the depairing current at the indicated temperature.

Sample ID	Width μm	Length μm	$R_s(300\text{ K})$ Ω/sq	$I_c(1.7\text{ K})$ μA	$I_{\text{dep}}(1.7\text{ K})$ μA	$I_c/I_{\text{dep}}(1.7\text{ K})$
2–2	0.19	2.2	574	45.2	52.5	0.8 – 0.9
2–4	1.02	8.4	564	242.5	284	0.8 – 0.9
2–11	1.95	23.9	580	458	528	0.8 – 0.9
2–6	3.00	30.6	584	705	806	0.8 – 0.9

To build probability density function, we measure the time delay between the trigger pulse from the laser and the corresponding electrical pulse from the sample using Time Tagger Ultra by Swabian Instruments with 12-ps resolution. To build one PDF we accumulate $10^4 - 10^5$ pairs of pulses. We set the trigger threshold of each channel (sample channel and laser trigger channel) at 50% of the corresponding signal amplitude to minimize the contribution of the amplitude fluctuations. We use a fast photodiode instead of SMSPD to measure optical jitter τ_o, which includes laser + fibers + time tagger, $\tau_o = 25$ ps. We follow Ref. [11] to estimate noise jitter τ_n, which is a contribution from the amplifier noise: $\tau_n = \sigma U_N \times \tau_r / A_{\text{mean}}$, where σU_N is the rms of the voltage transient at the baseline, τ_r is the rise time, and A_{mean} is the average amplitude of the photocount voltage pulse of the detector. The narrowest strip ($w = 0.19$ μm) has the smallest current and thus the smallest magnitude of the voltage pulse. This results in $\tau_n = 39$ ps at current close to I_c and increases up to 66 ps when the current decreases. All other samples, which are SMSPD, have much larger magnitude of the voltage pulse, which results in τ_n not higher than 15 ps. The instrumental jitter $\tau_{\text{inst}} = \sqrt{\tau_o^2 + \tau_n^2}$ is in the range 46–71 ps for the narrowest sample, and about 29 ps for SMSPDs [color solid lines in Fig. 2(a)].

In Fig. 1 we show probability density function of our detectors at different currents corresponding to $\eta = 0.2$, 0.5, 0.95, and at $I \approx I_c$ [dependnece of $\eta(I)$ is shown in Fig. 2(b)]. One can see that PDF is non-Gaussian-like as in the case of nanostrips [9–12] but in addition we observe oscillations for wide microstrips and low currents. We check that their presence is not connected with possible reflections in our measurement setup: we vary the distance between the tip of the ferrule and the sample in the range 1–10 cm, and varied the distance between the position of shunt resistor and the sample in the range 0.2–7 cm. In both cases we do not observe any significant influence on the period of PDF oscillations and the presence of the "shoulders."

In Fig. 2(a) we present the current dependence of the timing jitter, which is determined as the FWHM of PDF. In the case of the narrowest strip (0.19 μm), the timing jitter decreases with the increase of the current, as in the case of SNSPD, and reaches a value limited by the instrumental jitter (black solid line for the strip width 0.19 μm, and colored lines for other widths).

For SMSPDs ($w \geq 1$ μm), jitter experiences a noticeable increase in a region where internal detection efficiency η changes rapidly with current. At these currents, PDF has essentially non-Gaussian shape with a noticeable "shoulder" (and sometimes oscillations) leading to the increase of PDF width taken at half of its maximum.

Near critical current jitter reaches its minimum value. The straight lines in Fig. 2(a) denote instrumental contribution to the jitter of the studied sample. For the narrowest sample, the instrumental jitter is the highest one equal to 46 ps due to low amplitude of the voltage pulse from the

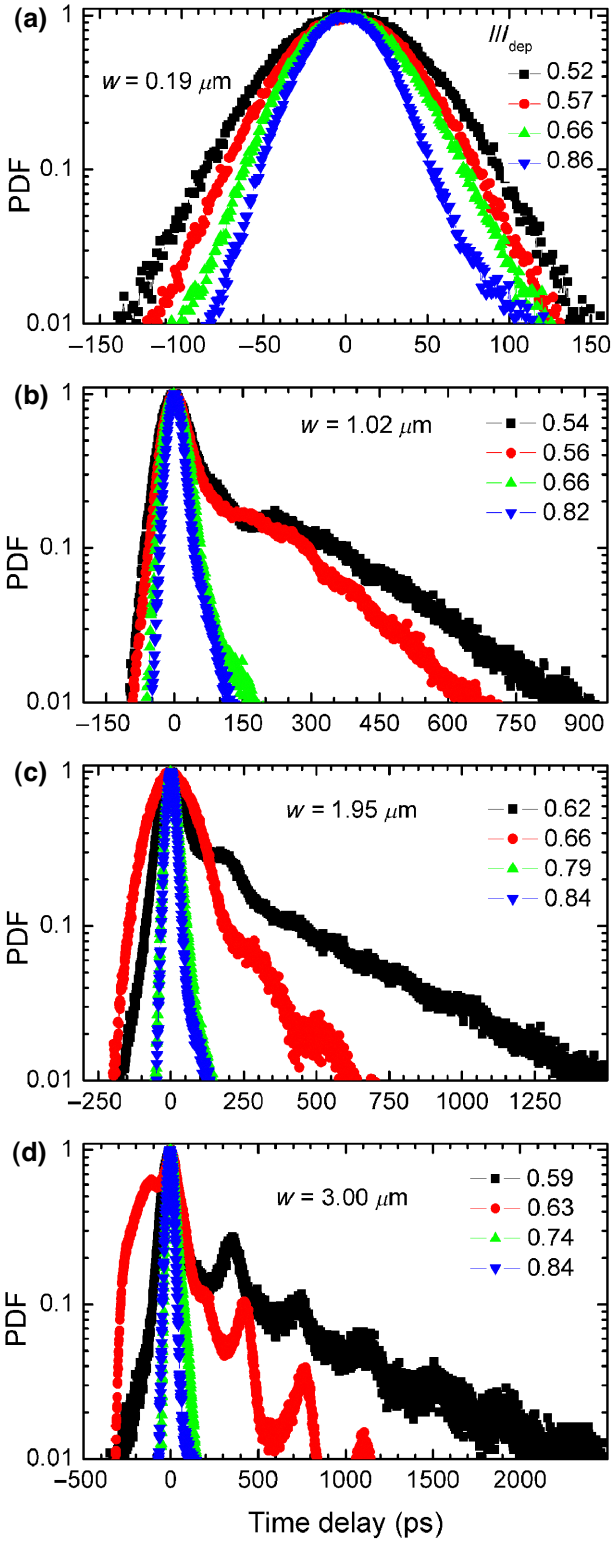

FIG. 1. Probability density function for NbN strips with different widths found at different currents corresponding to $\eta = 0.2$, 0.5, 0.95, and $I \approx I_c$ [see Fig. 2(b)].

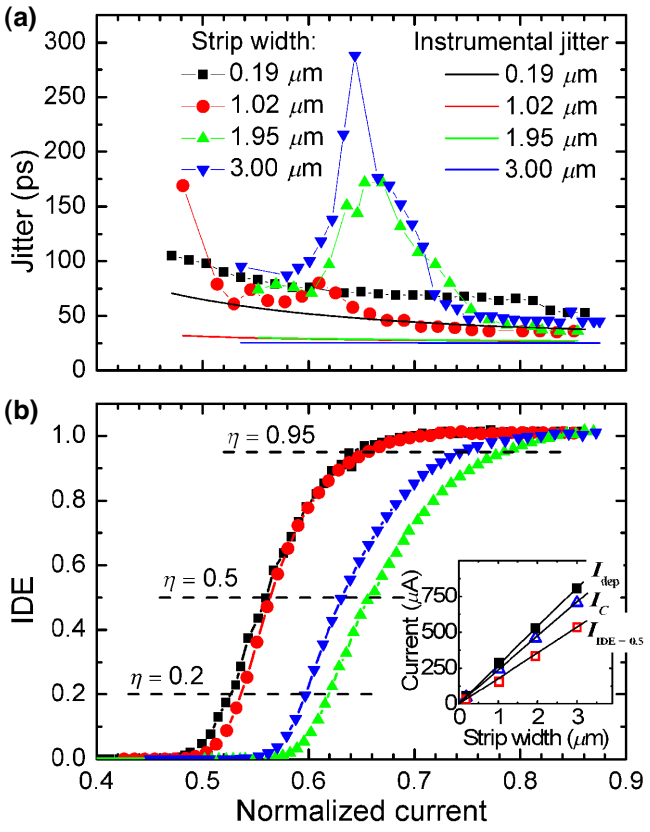

FIG. 2. (a) Dependence of the timing jitter and (b) dependence of internal detection efficiency η on normalized bias current $I/I_{\rm dep}$. Black line in (a) is the instrumental jitter for the narrowest sample, colored lines are the instrumental jitter for all other samples. The higher level of the instrumental jitter of the narrowest sample is caused by the small current of the sample resulting in small magnitude of voltage pulse. Dashed lines in (b) denote IDE levels of 0.2, 0.5, and 0.95. The IDE curves are not placed monotonously from left to right according to strip width. This is the consequence of not having sufficient accuracy in sample current measurement. Although it does not affect our results concerning jitter. The inset shows depairing current $I_{\rm dep}$, measured critical current I_c, and current corresponding to IDE = 0.5 ($I_{\rm IDE\,=\,0.5}$ for samples of different width. Good linear dependencies confirm that the samples do not have any noticeable defects.

detector (due to its small current). With the total jitter of 50 ps, this gives intrinsic jitter of 19.6 ps. For SMSPD instrumental jitter is at a level of 29 ps giving intrinsic jitter of 24 ps for 1- and 2 $-$ μm-wide samples, and 28 ps for the 3 $-$ μm-wide sample.

One may notice that detection efficiency curves are not placed monotonously according to the strip width increase. We attribute it to the following reasons: (1) we use a shunt resistor to avoid latching. In this case the current measured by the source is split between the shunt and the strip (due to the presence of normal contacts to the sample). We cannot measure accurately enough the ratio of the currents in the sample and in the shunt, causing a small arbitrary shift of the detection curve to the left or right; (2) the samples may have some minor variation in quality causing small variation of the current at which the sample starts detecting photons. Meanwhile, to confirm that all our samples are of the same quality we plot (see inset) the relevant currents (i.e., depearing current, critical current, and current corresponding to $\eta = 0.5$) versus strip width demonstrating clear linear dependencies.

In Fig. 1 one can see that the PDF is much broader for micron-wide strips at low currents (when $\eta \ll 1$) than for the narrow one. Besides, at the currents corresponding to the same level of η, the broadness of PDF increases with increasing w. Our calculations presented below may explain this effect by increased time to cross the strip by first vortex, which gives a large contribution to the delay time.

III. RESULTS OF THEORETICAL CALCULATIONS

To calculate delay time and its variance we use the same model as in Refs. [2,15] where single-photon response of the wide strip was predicted and intrinsic timing jitter of the narrow strip (with width about 100 nm) was studied. The model consists of the modified time-dependent Ginzburg-Landau equation, which describes dynamics of the superconducting order parameter and equations for time and space evolution of electron and phonon temperatures. To compare our results with the case of narrow strip we use the same temperature ($T = 0.5T_c$) and material parameters as in Ref. [15], which are close to parameters of the NbN microstrips studied here. We do not expect that our model is able to fit quantitatively our experimental results (due to its limitations—see discussion in Refs. [2,15]) but it takes into account important physical "ingredients" of the studied problem: the appearance of a hotspot and its evolution in time, suppression of superconducting order parameter Δ inside the hotspot, current crowding effect near the hotspot, nucleation of vorticies inside the hotspot, or at the edge of the strip—depending on the position of the hotspot in the strip, current-induced vortex motion, vortex-vortex and vortex-antivortex interaction in the strip, interaction of vortices and antivortices with edges, finite relaxation time of Δ in the hotspot and in the vortex path, Joule dissipation. The list of these necessary "ingredients" demonstrates the complexity of the studied problem. Our aim is to see what this model predicts and its relation with our experimental observations.

Using the energy conservation law we estimate the diameter of the photon-induced hotspot (assuming $T = T_c$ inside the hotspot—see Eq. (38) in [2]) for our material parameters and the wavelength 1064 nm (photon energy approximately 1.2 eV) as $D_{\rm HS} = 54$ nm $\simeq 8.6\xi_c$ [$\xi_c = (\hbar D/k_B T_c)^{1/2} \simeq 6.3$ nm for our NbN]. In modeling we

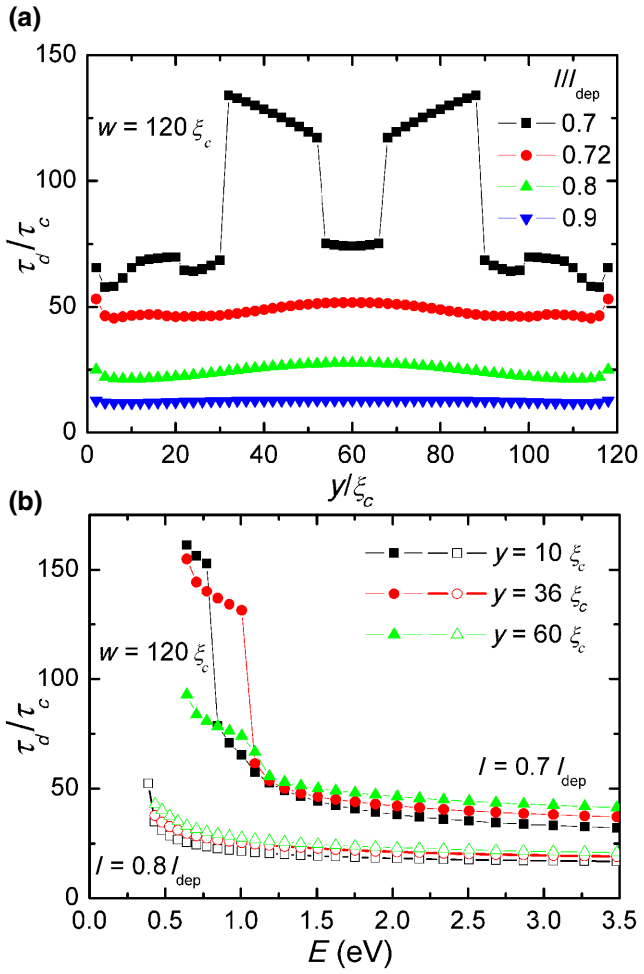

FIG. 3. (a) Position-dependent delay time in the strip with width $w = 120\xi_c$ calculated at different currents (bath temperature $T = 0.5T_c$ and photon energy $E = 1$ eV). (b) Dependence of τ_d on deposited energy for three photon-absorption sites $y = 10, 36, 60\xi_c$ and two values of the current ($\tau_c = \hbar/k_BT_c$).

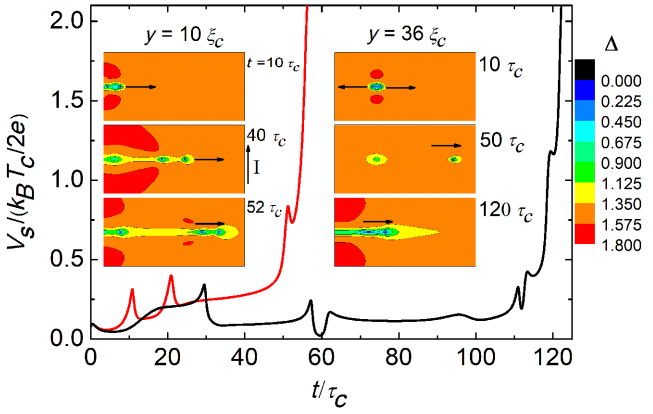

FIG. 4. Time dependence of the voltage drop along the superconducting strip (time is normalized in units of $\tau_c = \hbar/k_BT_c$) after absorption of the photon at different sites $y = 10\xi_c$ (red curve) and $y = 36\xi_c$ (black curve) across the strip with width $120\xi_c$. In the insets we show the snapshots of the superconducting order parameter at different times. Current $I = 0.7I_{\rm dep}$, $T = 0.5T_c$, $E = 1$ eV. The yellow region corresponds to the channel with a suppressed order parameter. Red color corresponds to the largest Δ. Two red regions appear because current deviates from the hot region and locally Δ becomes larger (current density locally goes down). At $50\tau_c$ (in the case of $y = 36\xi_c$, black curve), Δ partially recovers in the hotspot and locally current density is increased and Δ goes down. At the moment of time $t = 120\tau_c$, the channel with suppressed Δ appears at the left edge, superconducting current deviates, and Δ increases until two red regions appear again.

use different $w = 60, 120, 240\xi_c$ (they are much larger than $D_{\rm HS}$) to study how dynamic response depends on the width of the strip.

In Fig. 3 we present the position-dependent delay time in a strip with $w = 120\xi_c$. The main difference with the narrow strip [compare with Fig. 3(a) in Ref. [15]] is in the large variance of delay times at current $I = 0.7I_{\rm dep}$, which is just above the maximal detection current $I_{\rm det}^{\rm max} = 0.695I_{\rm dep}$ for photon with energy 1 eV (at $I > I_{\rm det}^{\rm max}$ all points across the strip participate in photon detection and theoretical detection efficiency saturates [2]). The main reason for this is complicated vortex dynamics in the strip with $w \gg D_{\rm HS}$ at relatively low currents. To demonstrate it in Fig. 4 we show voltage response when the photon is absorbed in different places across the strip (at $y = 10\xi_c$ and $36\xi_c$), which have large difference in τ_d—see Fig. 3(a).

When the photon is absorbed at $y = 10\xi_c$, after nucleation of the first vortex-antivortex pair at $t \simeq 10\tau_c$ ($\tau_c = \hbar/k_BT_c$), the second pair is nucleated in the hotspot before the first vortex exits the strip via the farthest edge located at $y = 120\xi_c$ (the first antivortex exits faster via the nearest edge). It occurs because in the hotspot region Δ is still suppressed, the antivortex already left the strip while the first vortex is far enough and weakly influences the nucleation of the second pair (when it is close it forbids its nucleation). It leads to relatively fast creation of the channel (having yellow color in the inset in Fig. 4) with suppressed order parameter because the second vortex moves along the path created by the first vortex, where Δ is partially suppressed with larger velocity. This channel then develops to a growing normal domain at $t \simeq 60\tau_c$. We call such a photon-absorption site, which leads to the relatively fast appearance of this channel, a "fast" site.

In contrast, when the photon is absorbed at $y = 36\xi_c$, the next vortices and antivortices do not appear until the first vortex exits via the farthest edge. It occurs because the first antivortex exists later than at $y = 10\xi_c$, the order parameter in the hotspot recovers stronger and the first vortex forbids nucleation of the second vortex-antivortex pair. In this case, the next vortices and antivortices enter the strip

via edges, in the place where previous vortex and antivortex exits (in that place Δ is suppressed larger than in other places along the edge due to the passed vortex). It leads to a longer delay in the appearance of the channel with suppressed Δ. We call the photon-absorption site, which leads to such a dynamics, a "slow" site.

From a physical point of view, this different dynamics is a result of competition between the relaxation time of Δ in the hotspot, in a wake behind the moving vortex, intervortex interaction, and interaction of vortices with the current and edges of the strip. We find similar behavior for strips with $w = 60\xi_c$ and $240\xi_c$ at $I \sim I_{\rm det}^{\rm max}$. There are "slow" and "fast" sites with the only difference that in the narrower strip, the variance in delay times is smaller, while in the wider strip it is larger. It happens due to the increase of delay time in "slow" sites with increasing w due to the longer flight time of the first vortex across the strip. Delay time in "fast" sites also increases but smaller because the second pair is nucleated and the second vortex moves with large velocity along the "trench" in Δ created by the first vortex (see the middle inset at $y = 10\xi_c$ in Fig. 4).

In the narrow strip with $w \sim D_{\rm HS}$ the order parameter is suppressed inside the hotspot and, hence, almost across the whole strip. It favors fast vortex motion, the order parameter does not have time to recover, and passage of the first vortices creates the channel with a suppressed order parameter. As a result position-dependent variance in delay time is relatively small even at $I \sim I_{\rm det}^{\rm max}$ [see Fig. 3(a) in Ref. [15]].

With increasing current (for the chosen parameters already at $I = 0.72 I_{\rm dep}$ for strip with $w = 120\xi_c$) the variance in time delay becomes much smaller [see Fig. 3(a)]. At this and larger currents, the second generation of vortices is nucleated before the exit of the first one at any absorption site and it equalizes the delay times. With increasing current the vortices and antivortices move faster, their nucleation time decreases, and it leads to decreasing of both τ_d and its variance. The same occurs in strips with $w = 60\xi_c$ and $120\xi_c$.

With calculated dependence $\tau_d(y, E)$ at different currents [its example is shown in Fig. 3(b)] we can find PDF for different widths of the strip and energy of the photon. To do it, we use the same procedure as in Ref. [15]. Namely we introduce weight factor

$$P(E) = \frac{1}{\sigma\sqrt{2\pi}} e^{-(E-\bar{E})^2/2\sigma^2}, \qquad (2)$$

which describes fluctuations in the deposited electron energy after absorption of the photon ($\bar{E}$ is the most probable deposited energy and σ is deviation from the mean value) [15,16,22]. Alternatively, one may assume that material parameters of the microstrip vary in space, at fixed deposited energy, leading to variations of $I_{\rm det}$. Then we convert dependence $\tau_d(y, E)$ to $E(\tau_d, y)$, insert it to Eq. (1), and average $P(\tau_d, y)$ over the width. In calculations we choose $\bar{E} = 1$ eV and $\sigma = 0.1\bar{E}$.

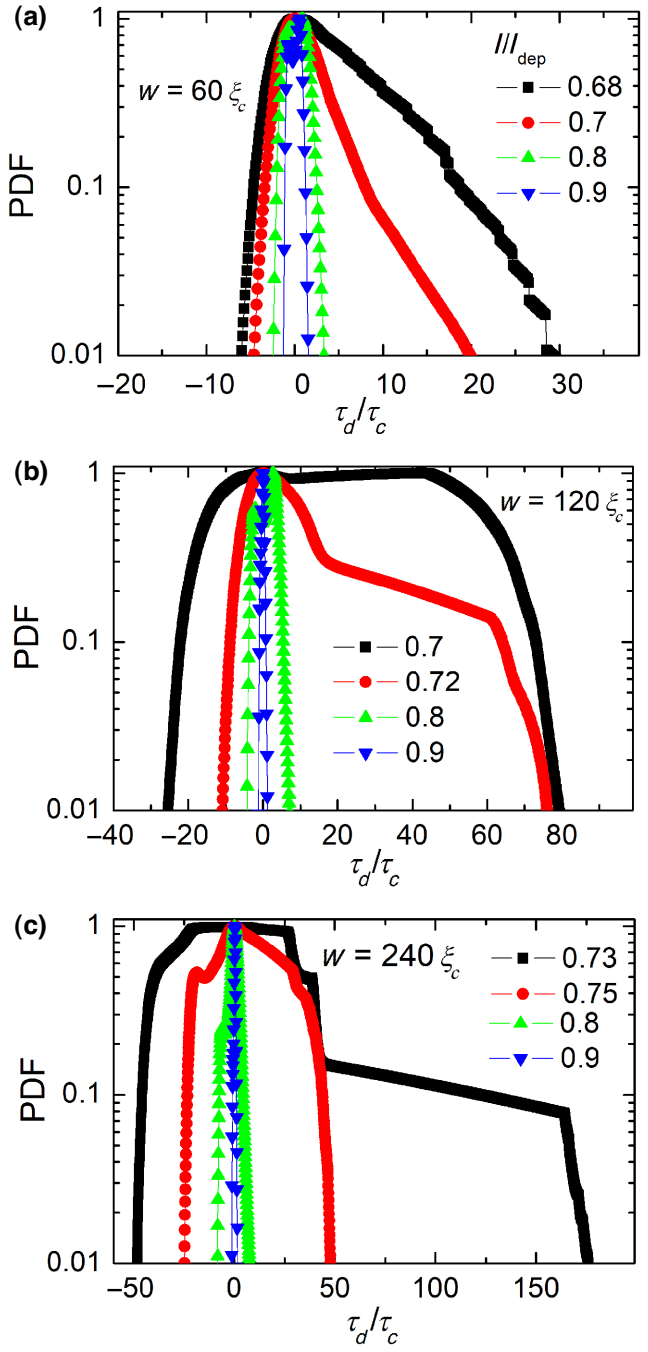

FIG. 5. Probability density function calculated for different currents and widths. In calculations we choose $\bar{E} = 1$ eV and $\sigma = 0.1\bar{E}$, which roughly corresponds to photons with energy 1.1–1.2 eV. The best jitter values that we measure at currents near I_c, are in the range from 19.6 ps (for 0.19 μm strip) to 28 ps (for 3-μm-wide strip), which correspond to $23\tau_c - 36\tau_c$.

Our results for normalized PDF $\sim \int P(\tau_d, y)dy$ are present in Fig. 5. Qualitatively, they resemble experimental PDF, namely the presence of the shoulder and increase

of its width with increasing of w and decrease of timing jitter with increasing of the current. In our model, the shoulder is connected with position-dependent vortex dynamics leading at low currents to rather different delay times for photons absorbed in different sites in the strip [see Fig. 3(a)] and with increasing w this difference increases. In the narrow strip, a small shoulder is also present (see Fig. 6 in Ref. [15]) where it is also connected with position-dependent vortex dynamics but with a smaller difference in delay times.

Close comparison between theory and experiment shows quantitative difference. For example, for a strip with $w = 240\xi_c \simeq 1.5$ μm, the width of the shoulder is about $200\tau_c \sim 200$ ps, which is much smaller than a nanosecond [see Figs. 1(b) and 1(c)]. This difference can be connected with assumed in our model very small electron-electron inelastic scattering time $\tau_{e-e}(T)$. This assumption is valid at the initial stage of hotspot formation but not at large times, when electron temperature is close to bath temperature [2]. Short τ_{e-e} speeds up the relaxation time of the superconducting order parameter and vortex motion [23] while large τ_{e-e} slows it down and considerably increases the delay time. It can explain the large difference between the experimental and theoretical width of the shoulder in PDF. But to take into account the effect of large τ_{e-e} quantitatively one has to solve a kinetic equation instead of a heat-diffusion equation, which is a rather complicated problem.

Our theory also predicts the decrease of timing jitter and the width of the shoulder with increasing current (a similar result was found for the narrow strip [15]). Indeed, even a small increase of the current makes timing jitter much smaller because new vortices appear before the first ones exit the strip and, besides, they move much faster. We have to stress, that at currents not far from depairing current vortex velocity depends on current nonlinearly (it could be seen from Fig. 3, because the flight time of the first vortex across the strip gives a large contribution to the delay time and its dependence on current). As in the narrow strip [15], timing jitter approaches $\hbar/k_BT_c$ as $I \to I_{\rm dep}$. We believe that such a drastic decrease of timing jitter has not been observed in our experiment because of relatively large instrumental jitter [due to the same reason, the dependence of timing jitter on width is visible only at low currents—see Fig. 2(a)]. Note also, that in calculations we take substrate temperature $T = 0.5T_c$, which leads to $I_{\rm det}^{\rm max} \simeq 0.7I_{\rm dep}$ [2]. At lower temperatures $I_{\rm det}^{\rm max}$ approaches $0.5I_{\rm dep}$ as $T \to 0$ (see Fig. 8 in Ref. [3]), which is close to current when single-photon detection is observed in Refs. [5,6] and in our experiment [see Fig. 2(b)] with $T = 0.19T_c$.

In the framework of our model we do not find oscillations of PDF. We speculate that it could be connected with our assumption that current in the strip does not change. In the experiment, nucleation and motion of vortices leads to resistive state. It means that current in the strip should decrease during vortex motion because there is a shunt in our setup. But decrease of current slows down the vortex motion, and, hence, corresponding resistance. Therefore, in our system consisting of the superconducting strip and the shunt, the oscillations of the current may occur. Their period should depend of kinetic inductance of the strip, its width and current, because time flight of vortex across the strip depends on w and current. Indeed, from Fig. 1 one can see that the period of oscillations depends on current and they are more visible for wider strips. But solid proof of this idea is possible only by studying strips with different kinetic inductance (i.e., different length-to-width ratio).

IV. CONCLUSION

We experimentally find that at large currents, where internal detection efficiency saturates, timing jitter in photon detection increases slowly with the strip width from 19.6 ps for a width of 0.19 μm to 28 ps for a width of 3 μm. At low currents we find that the probability density function becomes broader with the increase of the strip width. Our calculations in the framework of the time-dependent Ginzburg-Landau equation and two-temperature model indicate that the last effect could be connected with complicated vortex dynamics leading to position-dependent vortex dynamics and the existence of "fast" and "slow" absorption sites across the superconductor. The model also predicts that intrinsic timing jitter for a micron-wide strip could be as small as $\hbar/k_BT_c$ as one approaches the depairing current.

ACKNOWLEDGMENTS

We acknowledge Ph. Zolotov for the NbN film deposition. We thank Swabian Instruments GmbH and Dr. Helmut Fedder personally for the kindly provided experimental equipment (Time Tagger Ultra 8). The work is supported by the Russian Science Foundation (RSF), Grant No. 20-12-00287 (in part concerning theoretical study of delay time) and by the Russian Foundation for Basic Research (RFBR), Grant No. 18-29-20100 (in part, concerning experimental study of delay time).

[1] G. N. Goltsman, O. Okunev, G. Chulkova, A. Lipatov, A. Semenov, K. Smirnov, B. Voronov, and A. Dzardanov, Picosecond superconducting single-photon optical detector, Appl. Phys. Lett. **79**, 705 (2001).

[2] D. Yu. Vodolazov, Single-Photon Detection by a Dirty Current-Carrying Superconducting Strip Based on the Kinetic-Equation Approach, Phys. Rev. Appl. **7**, 034014 (2017).

[3] Y. Korneeva, D. Vodolazov, A. Semenov, I. Florya, N. Simonov, E. Baeva, A. Korneev, G. Goltsman, and T. Klapwijk, Optical Single-Photon Detection in Micrometer-Scale NbN Bridges, Phys. Rev. Appl. **9**, 64037 (2018).

[4] Yu. P. Korneeva, N. N. Manova, I. N. Florya, M. Yu. Mikhailov, O. V. Dobrovolskiy, A. A. Korneev, and D. Yu. Vodolazov, Different Single-Photon Response of Wide and Narrow Superconducting $Mo_xSi_1 - x$ Strips, Phys. Rev. Appl. **13**, 024011 (2020).

[5] I. Charaev, Y. Morimoto, A. Dane, A. Agarwal, M. Colangelo, and K. K. Berggren, Large-area microwire MoSi single-photon detectors at 1550 nm wavelength, arXiv:2020.09088.

[6] J. Chiles, S. M. Buckley, A. Lita, V. B. Verma, J. Allmaras, B. Korzh, M. D. Shaw, J. M. Shainline, R. P. Mirin, and S. W. Nam, Superconducting microwire detectors with single-photon sensitivity in the near-infrared, Appl. Phys. Lett. **116**, 242602 (2020).

[7] J. Zhang, W. Slysz, A. Pearlman, A. Verevkin, R. Sobolewski, O. Okunev, G. Chulkova, and G. N. Goltsman, Time delay of resistive-state formation in superconducting stripes excited by single optical photons, Phys. Rev. B **67**, 132508 (2003).

[8] N. Calandri, Q.-Y. Zhao, D. Zhu, A. Dane, and K. K. Berggren, Superconducting nanowire detector jitter limited by detector geometry, Appl. Phys. Lett. **109**, 152601 (2016).

[9] M. Sidorova, A. Semenov, H.-W. Hubers, I. Charaev, A. Kuzmin, S. Doerner, and M. Siegel, Physical mechanisms of timing jitter in photon detection by current-carrying superconducting nanowires, Phys. Rev. B **96**, 184504 (2017).

[10] M. Caloz, M. Perrenoud, C. Autebert, B. Korzh, M. Weiss, Ch. Schonenberger, R. J. Warburton, H. Zbinden, and F. Bussieres, High-detection efficiency and low-timing jitter with amorphous superconducting nanowire single-photon detectors, Appl. Phys. Lett. **112**, 061103 (2018).

[11] M. Sidorova, A. Semenov, H.-W. Hubers, A. Kuzmin, S. Doerner, M. Siegel, and D. Vodolazov, Timing jitter in photon detection by straight superconducting nanowires: Effect of magnetic field and photon flux, Phys. Rev. B **98**, 134504 (2018).

[12] Misael Caloz, B. Korzh, E. Ramirez, Ch. Schonenberger, R. J. Warburton, H. Zbinden, M. D. Shaw, and F. Bussieres, Intrinsically-limited timing jitter in molybdenum silicide superconducting nanowire single-photon detectors, J. Appl. Phys. **126**, 164501 (2019).

[13] B. Korzh *et al.*, Demonstration of sub-3 ps temporal resolution with a superconducting nanowire single-photon detector, Nat. Photonics **14**, 250 (2020).

[14] H. Wu, Ch. Gu, Yu. Cheng, and X. Hu, Vortex-crossing-induced timing jitter in superconducting nanowire single-photon detectors, Appl. Phys. Lett. **111**, 062603 (2017).

[15] D. Yu. Vodolazov, Minimal Timing Jitter in Superconducting Nanowire Single-Photon Detectors, Phys. Rev. Appl. **11**, 014016 (2019).

[16] J. P. Allmaras, A. G. Kozorezov, B. A. Korzh, K. K. Berggren, and M. D. Shaw, Intrinsic Timing Jitter and Latency in Superconducting Nanowire Single-Photon Detectors, Phys. Rev. Appl. **11**, 034062 (2019).

[17] J. Zichi, J. Chang, S. Steinhauer, K. von Fieandt, J. W. Los, G. Visser, N. Kalhor, T. Lettner, A. W. Elshaari, Ali W. Zadeh, Iman Esmaeil, and V. Zwiller, Optimizing the stoichiometry of ultrathin NbTiN films for high-performance superconducting nanowire single-photon detectors, Opt. Express **19**, 26579 (2019).

[18] V. Shcheslavskiy, P. Morozov, A. Divochiy, Yu. Vakhtomin, K. Smirnov, and W. Becker, Ultrafast time measurements by time-correlated single photon counting coupled with superconducting single photon detector, Rev. Sci. Instrum. **87**, 053117 (2016).

[19] K. Smirnov, A. Divochiy, Yu. Vakhtomin, P. Morozov, Ph. Zolotov, A. Antipov, and V. Seleznev, NbN single-photon detectors with saturated dependence of quantum efficiency, Supercond. Sci. Technol. **31**, 035011 (2018).

[20] John R. Clem and V. G. Kogan, Kinetic impedance and depairing in thin and narrow superconducting films, Phys. Rev. B **86**, 174521 (2012).

[21] S. Frasca, B. Korzh, M. Colangelo, D. Zhu, A. E. Lita, J. P. Allmaras, E. E. Wollman, V. B. Verma, A. E. Dane, E. Ramirez, A. D. Beyer, S. W. Nam, A. G. Kozorezov, M. D. Shaw, and K. K. Berggren, Determining the depairing current in superconducting nanowire single-photon detectors, Phys. Rev. B **100**, 054520 (2019).

[22] A. G. Kozorezov, C. Lambert, F. Marsili, M. J. Stevens, V. B. Verma, J. P. Allmaras, M. D. Shaw, R. P. Mirin, and Sae Woo Nam, Fano fluctuations in superconducting-nanowire single-photon detectors, Phys. Rev. B **96**, 054507 (2017).

[23] D. Yu. Vodolazov and F. M. Peeters, Temporary cooling of quasiparticles and delay in voltage response of superconducting bridges after abruptly switching on the supercritical current, Phys. Rev. B **90**, 094504 (2014).